

HYDROTHERMAL STABILITY RELATIONS OF  
SYNTHETIC LEPIDOLITEJ. L. MUNOZ, *Department of Geological Sciences, University of  
Colorado, Boulder, Colorado 80302*

## ABSTRACT

The hydrothermal stability relations of two trioctahedral lepidolite end members—polyolithionite ( $\text{KLi}_2\text{AlSi}_4\text{O}_{10}\text{F}_2$ ) and trillithionite ( $\text{KLi}_{3/2}\text{Al}_{3/2}\text{Si}_3\text{AlO}_{10}(\text{F},\text{OH})_2$ )—have been determined as a function of total fluid pressure (up to 2 kbar) and temperature (up to the liquidus) both in the presence and absence of excess quartz. The fugacity of  $\text{HF}$  ( $f_{\text{HF}}$ ) was fixed by the bulk composition of the charges and by the rate of decomposition of the lepidolite; in most experiments in which lepidolite was completely decomposed,  $f_{\text{HF}}$  was high: on the order of 10 to 100 bars.

Under these conditions, polyolithionite melts congruently at  $770 \pm 15^\circ\text{C}$ , 2 kbar, whereas trillithionite melts incongruently forming eucryptite ( $\text{LiAlSiO}_4$ ) + liquid at  $678 \pm 15^\circ\text{C}$ , 2 kbar. At lower total pressures, the stabilities of both micas are slightly reduced and the decomposition reactions change: below about 1.5 kbar,  $760^\circ\text{C}$ , polyolithionite melts incongruently to sanidine + liquid; below 1.1 kbar,  $675^\circ\text{C}$ , trillithionite reacts to form eucryptite + leucite + kalsilite + gas. For both micas, decreasing  $f_{\text{HF}}$  relative to  $f_{\text{H}_2\text{O}}$  at constant total pressure lowers the maximum thermal stability and raises the solidus. The result of these two effects is to displace melting relations to higher pressures and temperatures; for example, if  $f_{\text{HF}} \approx 1$  bar, subsolidus decomposition will occur for both micas at 2 kbar.

Polyolithionite is indifferent to the presence of excess quartz, but the stability of trillithionite is markedly lowered by coupling reactions with  $\text{SiO}_2$ . At 2 kbar, the maximum stability of the assemblage trillithionite + quartz ranges from as low as  $400^\circ\text{C}$  up to  $530^\circ\text{C}$  as  $\text{O}_{\text{H}0}$  varies from about 0.001 bar to about 10 bars.

Lepidolite commonly occurs as a relatively late stage (subsolidus) mineral in lithium-bearing granitic pegmatites. The late appearance of lepidolite in the evolution of pegmatite assemblages reflects the restriction of lepidolite stability in these environments to low temperatures. This may be explained either by the ubiquitous presence of quartz in these rocks or by a relatively low  $f_{\text{HF}}$  during the magmatic stage of crystallization. Much lepidolite may form by subsolidus reaction of spodumene and potash feldspar in the presence of a fluorine-bearing aqueous gas.

## INTRODUCTION

Lepidolite (lithium-rich aluminous mica) is commonly found in granitic pegmatites. The petrogenesis of these "lithium pegmatites" has aroused much interest, probably because of their unusual textures, enrichment in trace elements, and economic importance (Cameron *et al.*, 1949; Jahns, 1955). This paper describes the hydrothermal stability relations of the two most important lepidolite end members and provides a model for the study of phase relations involving lepidolite in natural systems.

Stability relations of synthetic lepidolite were studied in the system K-Li-Al-Si-F-O-H. Figure 1 shows the compositions of the important crystalline phases in the condensed system  $\text{KAlSiO}_4\text{-Li}_2\text{SiO}_3\text{-Al}_2\text{O}_3\text{-SiO}_2$ . The compositions of idealized iron-free lepidolite lie on a plane inside the

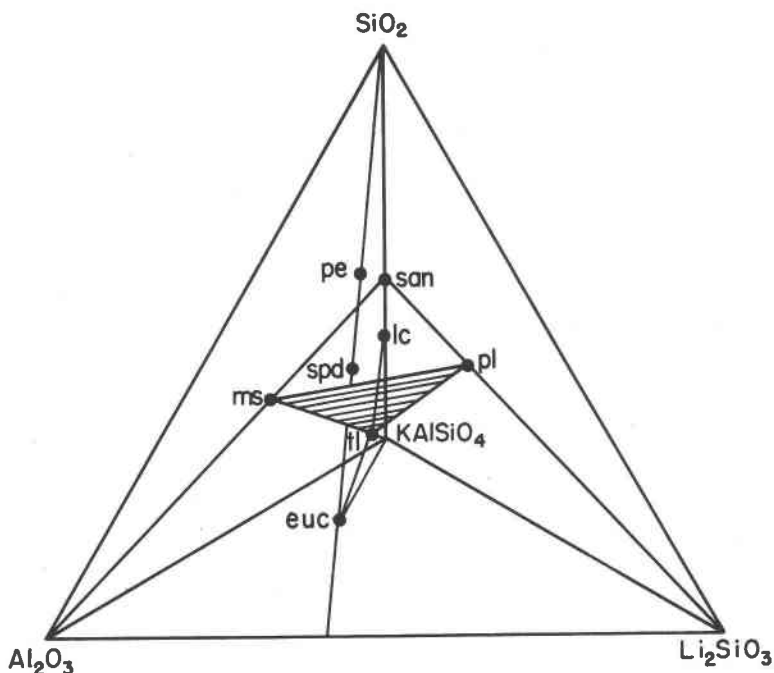


FIG. 1. Chemographic positions of phases encountered in this study plotted in the condensed system  $\text{KAlSiO}_4\text{-Li}_2\text{SiO}_3\text{-Al}_2\text{O}_3\text{-SiO}_2$ . Compositions of micas are projected from imaginary OH and F apices onto the appropriate planes. Iron-free lepidolites lie on the shaded triangle PL-TL-MS. PL: polyolithionite, TL: trilithionite, MS: muscovite, Euc: eucryptite, Spd: spodumene, Pe: petalite, Lc: leucite, San: sanidine. See text or appendix for compositions of phases.

tetrahedron bounded by the compositions  $\text{KLi}_2\text{AlSi}_4\text{O}_{10}\text{F}_2$  (polyolithionite, PL),  $\text{KLi}_{3/2}\text{Al}_{3/2}\text{Si}_3\text{Al}_2\text{O}_{10}(\text{F},\text{OH})_2$  (trilithionite, TL), and  $\text{KAl}_2\text{Si}_3\text{AlO}_{10}(\text{OH})_2$  (muscovite, MS). The two lithium-bearing end members are trioctahedral micas; lepidolites can thus be expressed as ternary solutions of these two trioctahedral end members with muscovite, although the amount of MS in solid solution is usually less than 20 percent<sup>1</sup> (Foster, 1960; Munoz, 1968, p. 1491). Thus PL and TL represent idealized lepidolite end member compositions; for this reason, the stability relations of these bulk compositions were investigated. In a previous publication (Munoz, 1968), solid solution in both natural lepidolites and in the synthetic ternary system PL-TL-MS has been discussed in detail.

<sup>1</sup> In this paper, lithium micas which have the  $2M_1$  muscovite structure and which contain more than 25 percent of the MS component in solid solution are not considered to be lepidolite.

## EXPERIMENTAL PROCEDURES AND TECHNIQUES

Standard hydrothermal procedures were followed during this investigation. Run materials were sealed in gold or platinum capsules. A few experiments were performed using the fluorine buffer technique (Munoz and Eugster, 1969). Experiments were accomplished in stellite "cold seal" rod bombs which were externally heated. Chromel-alumel thermocouples calibrated against the melting points of NaCl (800.5°C.) and Zn (419.5°C.) monitored the bomb temperature. Total fluid pressure was measured with a bourdon-tube gage which had been calibrated by the Heise Company to  $\pm 3$  bars. Runs were quenched either by lowering the pressure vessel into a bucket of cold water or by blowing compressed air onto the hot bomb.

All run products were X-rayed using powder diffractometer techniques and were analyzed optically. Descriptions of the physical properties of phases encountered during this study and information concerning preparation of starting materials appear in an appendix. Run tables from all stability experiments are deposited with the National Auxiliary Publication Service, American Society for Information Service.<sup>1</sup>

## STABILITY OF POLYLITHIONITE

Results of stability experiments for bulk compositions PL+H<sub>2</sub>O are shown in *P-T* projection (Fig. 2a). Polylithionite melts congruently above 1.5 kbar; at lower pressures the incongruent melting assemblage sanidine+liquid is observed. Interpretation of the results of experiments involving a liquid phase was complicated by the extreme reactivity of polylithionite glass. Thus, mica commonly formed during quenching. Moreover, heating a glass of polylithionite composition under hydrothermal conditions resulted in essentially total crystallization in the 30 minutes required to heat the bomb from room temperature to 800°C. For this reason, optical criteria were developed to determine whether a given polylithionite was in stable equilibrium at run conditions. For instance, stable micas commonly formed small (5–50  $\mu\text{m}$ ) clear euhedral platelets. Micas which formed by reaction with the gas phase were of giant size (up to 2 mm across) and contained many fluid inclusions. Micas in the process of melting showed ragged edges and contained copious glass inclusions. Even runs crystallized well below the solidus contained a small amount of glass (1–2 percent). This glass was commonly concentrated as tiny spheres near the cold end of the run capsule and most probably represents a quench from the aqueous gas phase.

The incongruent melting curve was easily detected because of the formation of sanidine in addition to abundant glass. In certain experiments at 0.5 kbar, lithium metasilicate appeared as a product along with sanidine and glass. This phase is almost certainly metastable under the

<sup>1</sup> To obtain a copy of this material, order NAPS Document Number 10609 from National Auxiliary Publications Service of the A.S.I.S., c/o CCM Information Corporation, 866 Third Avenue, New York, N.Y., 10022; remitting \$2.00 for microfiche or \$5.00 for photocopies, in advance, payable to CCMIC NAPS.

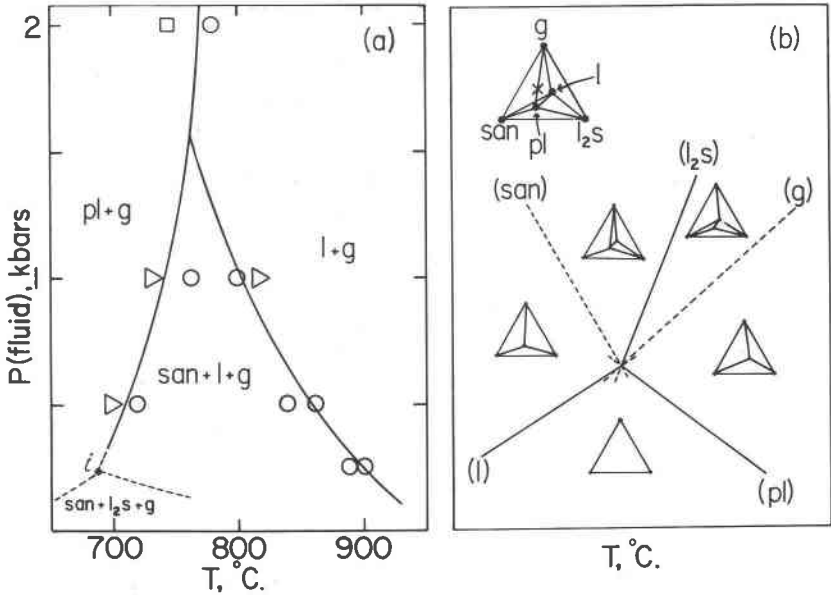


FIG. 2a (left).  $P$ - $T$  projection for polyolithionite+water showing curve-bracketing experiments only. Pl: polyolithionite, san: sanidine,  $l_2s$ : lithium metasilicate, l: liquid, g: gas. Starting materials: circles - polyolithionite+water, squares - glass+water, triangles - sanidine+glass+water. HF fugacity was fixed by the bulk composition of each experiment (see text). Dashed curves and invariant point  $san+l_2s+pl+l+g$  must exist at pressures below 500 bars, but were not detected experimentally.

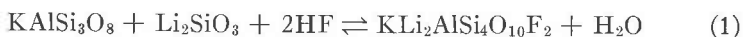
FIG. 2b (right). Analysis of sequence of univariant curves around the invariant assemblage  $pl+san+l_2s+l+g$ . (labelled i in 2a). The compositions of  $H_2O$  and HF have been projected along the same axis and are plotted as gas (g); the assemblage is invariant only for a fixed  $f_{HF}/f_{H_2O}$  ratio. The X in the chemographic insert (upper left) represents bulk composition  $pl+H_2O$ ; liquid composition is schematic. Dashed curves labelled (san) and (g) do not appear in 2a because they cannot be observed using  $pl+H_2O$  compositions.

conditions of these experiments because its appearance could be tied to capsules which had lost fluid or to bombs which were quenched unusually slowly in air. Replicate runs quenched rapidly in water did not yield lithium metasilicate.

Rigorous analysis of the above phase relations requires knowledge of the compositions of all phases, and this data is not available for the liquid and gas phases. However, certain limiting assumptions can be made. The fugacities of HF and  $H_2O$  were not buffered in these experiments but rather were defined by the bulk composition of the system. Each prepared capsule (solids+water) contained about 5 percent fluorine by weight in polyolithionite. Thus, in experiments which resulted in total decomposition of the mica, about 5 weight percent HF was avail-

able. By assuming ideal mixing in an HF-H<sub>2</sub>O gas phase, and by using fugacity coefficients for HF derived from critical constants (Hougen and Watson, 1946), one can calculate an (approximate!) fugacity of HF ( $f_{\text{HF}}$ ) of around 200 bars at 2 kbar 800°C. In terms of mole fractions, the H<sub>2</sub>O/HF ratio in the gas phase would be about 20:1. This calculation predicts only the *maximum*  $f_{\text{HF}}$ , since it is based on total decomposition of the mica, and on little or no fluorine in the liquid phase.<sup>1</sup>

The phase relations of PL+H<sub>2</sub>O can be best understood by reference to the reaction



This reaction, not observed in these experiments, represents the sub-solidus decomposition of polyolithionite. One possible explanation for not observing this reaction is that it may be stable only at relatively low

TABLE 1

$T, ^\circ\text{C}$	log K	log $f_{\text{HF}}$
627	18.16	-7.55
727	15.33	-6.09
827	13.08	-4.93

Approximate values of equilibrium constant ( $f_{\text{H}_2\text{O}}/f_{\text{HF}}^2$ ) and HF fugacity for the reaction  $\text{KAlSi}_3\text{O}_8 + \text{Li}_2\text{SiO}_3 + 2\text{HF} = \text{KLi}_2\text{AlSi}_4\text{O}_{10}\text{F}_2 + \text{H}_2\text{O}$  at a total fluid pressure of 2kbar. H<sub>2</sub>O fugacity is assumed to be that of the nickel-nickel oxide buffer in the system O-H. Thermodynamic data used in the calculations was taken from Robie and Waldbaum (1968).

$f_{\text{HF}}$ . This suggestion can be tested by calculating an approximate equilibrium constant for reaction (1) from free energy data, making the assumption that the free energy of formation of fluorophlogopite (Robie and Waldbaum, 1968) can be substituted for the free energy of polyolithionite. Furthermore, the equilibrium HF fugacity for the reaction can be calculated as a function of temperature, assuming that H<sub>2</sub>O fugacity is approximately that of the nickel-nickel oxide buffer in the system O-H. Results (TABLE 1) indicate that the assemblage sanidine + lithium metasilicate + gas should indeed be stable only at very low  $f_{\text{HF}}$ , especially in comparison to the experimental conditions actually

<sup>1</sup> The latter assumption is unrealistic, especially in view of the abundant quench crystals of LiF in the glass (see appendix). Nonetheless, arguments presented later in the section on trilithionite stability will demonstrate that HF fugacities obtained using the bulk composition method were certainly higher than those obtained in buffered experiments, where calculated HF fugacities range from about 0.01 to 10 bars. Thus realistic estimates of HF fugacities in unbuffered experiments should range from about 10 to 200 bars.

imposed. The hypothesis is further strengthened by noting that polyolithionite decomposes at 1 atm. in an open capsule, forming sanidine + lithium metasilicate; the reaction proceeds readily even below 700°C.

At constant total pressure, the assemblage polyolithionite + sanidine + lithium metasilicate + liquid + gas is invariant in  $f_{\text{HF}}-T$  space when plotted in the system  $\text{KAlSi}_3\text{O}_8\text{-Li}_2\text{SiO}_3\text{-HF-H}_2\text{O}$ . Alternatively, this assemblage is "invariant" in a  $P-T$  projection only for a fixed  $f_{\text{HF}}/f_{\text{H}_2\text{O}}$  ratio. This relationship has been shown schematically in Figure 2a (intersection of dashed curves) because its exact position is unknown; for  $f_{\text{HF}}/f_{\text{H}_2\text{O}}$  ratios imposed by these experiments, the invariant assemblage must lie below 500 bars. Finally, the sequence of univariant curves around the invariant point has been analyzed using Schreinemaker's technique (Fig. 2b).

Note that the intersection of the sanidine liquidus with polyolithionite stability in Figure 2a does *not* constitute an invariant assemblage; like any liquidus curve, the melting of sanidine in this system depends *both* on  $f_{\text{HF}}$  and  $f_{\text{H}_2\text{O}}$  as well as total pressure and temperature. Although, theoretically, a further increase in  $f_{\text{HF}}$  should lead to enlarging the stability field of polyolithionite (beyond that determined in these experiments), two counteracting effects will intervene. One of them is the depression of the liquidus due to increasing HF concentration (Wyllie and Tuttle, 1961) and the other is the increased solubility of polyolithionite in the gas phase as the acidity of the fluid is increased.

#### STABILITY OF TRILITHIONITE

The upper stability limit of trilitlionite is defined by the two reactions



Subsolidus decomposition occurs below 1.1 kbar over the temperature range 650–680°C. At higher pressures incongruent melting takes place at about 685°C, essentially independent of pressure. At higher temperatures, melting of kalsilite, leucite, and eucryptite is observed in turn (Fig. 3). The liquidus was located at 810°C at 2 kbar, and 840°C at 1 kbar, eucryptite being the liquidus phase.

At  $700 \pm 25$  bars and  $860 \pm 10^\circ\text{C}$ , the leucite reaction curve and eucryptite liquidus intersect, with both melting curves showing marked changes in slope. These relations are complicated by the inversion of eucryptite to its high temperature polymorph,  $\beta$ -eucryptite, a reaction which crosses the leucite liquidus very near this intersection. Isaacs and Roy (1958) determined the  $\alpha \rightleftharpoons \beta$  eucryptite inversion hydrothermally

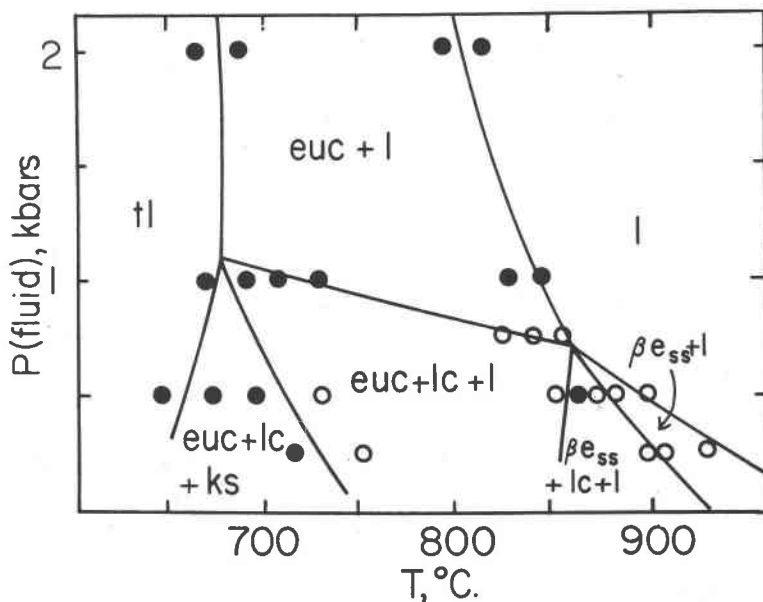


Fig. 3.  $P$ - $T$  projection for clithionite+water, showing positions of curve-bracketing experiments only. Dark circles enclosing a curve mean that the boundary was reversed; open circles mean that the position of the curve was determined by the reaction of trilitlionite. Because most assemblages involve a liquid, and reactions were rapid, even the non-reversed boundaries are probably very near equilibrium curves. Tl: trilitlionite, euc: eucryptite, lc: leucite, ks: kalsilite,  $\beta$ -e<sub>ss</sub>:  $\beta$ -eucryptite solid solution, l: liquid, g: gas. The fugacity of HF was fixed by the bulk composition of the charges (see text).

and, by projection, found that the transition should occur at  $848 \pm 5^\circ\text{C}$  at 1 atm. In the present investigation, only the conversion of  $\alpha$  to  $\beta$  was observed, the first trace of  $\beta$ -eucryptite forming at  $865^\circ\text{C}$  at 500 bars. This represents only an upper limit for the reaction, but fits well with Isaacs and Roy's data.

The sharp inflexion of the leucite reaction curve at the intersection of the eucryptite polymorphic inversion curve is most probably due to solid solution in  $\beta$ -eucryptite. Previous investigations of the systems  $\text{LiAlSiO}_4\text{-SiO}_2$  (Munoz, 1969), and  $\text{LiAlSiO}_4\text{-SiO}_2\text{-H}_2\text{O}$  (Roy *et al.*, 1950; D. B. Stewart, personal communication) indicate that extensive solid solution of  $\text{SiO}_2$  occurs in  $\beta$ -eucryptite, but not in eucryptite. The substitution of  $\text{Li}^+$  for  $\text{K}^+$ , or the coupled substitution  $\text{Li} + \text{Al} \rightleftharpoons \text{Si}$  in leucite is doubtful but unknown.

The two curves defining trilitlionite decomposition, and the two curves defining the melting of leucite and kalsilite, respectively, intersect at  $1.1 \pm 0.2$  kbar,  $678 \pm 15^\circ\text{C}$  (Fig. 3); the point represents the equilibrium

assemblage trillithionite+eucryptite+leucite+kalsilite+liquid+gas. At constant  $P_{\text{total}}$  and  $T$ , this is a possible invariant assemblage in the system  $\text{KAlSiO}_4\text{-LiAlSiO}_4\text{-SiO}_2\text{-HF-H}_2\text{O}$  if  $f_{\text{HF}}$  is independently variable (*i.e.*, buffered or externally defined). Because these experiments were carried out in the same way as the polyolithionite experiments, similar arguments apply regarding gas compositions: the fugacity of HF is determined by the bulk composition of the system and, after the mica has decomposed, is set at a relatively high level (on the order of tens to hundreds of bars). As the fugacity of HF is lowered relative to  $\text{H}_2\text{O}$ , two effects will be apparent at constant pressure: (1) the solidus should be displaced to higher temperatures, judging from results on the melting experiments in natural rock systems using HF- $\text{H}_2\text{O}$  mixtures (Jahns and Burnham, 1958); (2) the upper stability of trillithionite should be driven to lower temperatures. The net effect of these opposing trends will be to displace the equilibrium assemblage trillithionite+eucryptite+kalsilite+leucite+liquid+gas (invariant only for a particular  $f_{\text{HF}}/f_{\text{H}_2\text{O}}$  ratio) to higher pressures as seen in  $P\text{-}T$  projection; thus, at lower  $f_{\text{HF}}$ , one might anticipate subsolidus breakdown of trillithionite at 2 kbar and above. This hypothesis was tested by buffering trillithionite with the calcite-fluorite-graphite buffer (Munoz and Eugster, 1969) at 2 kbar, 620°C. This buffer imposes a calculated HF fugacity on the order of 0.5 bar under these conditions, which certainly must be lower than that obtained in unbuffered runs. After five weeks, the observed run products were eucryptite, leucite, and kalsilite (+unreacted trillithionite); no glass was present. This experiment provides confirmation of the predicted effect of HF on trillithionite stability. By analogy with arguments presented in the section on polyolithionite, the stability relations as determined in unbuffered experiments probably represent nearly the maximum hydrothermal stability of trillithionite.

#### STABILITY OF LEPIDOLITE+QUARTZ AT 2 KBAR

Because experimentally determined stability limits of individual minerals are only rarely directly applicable to complex geologic environments, the reaction of trioctahedral lepidolite with other phases was considered. The possible reaction of quartz with lepidolite is the most important coupling effect to determine, because quartz is almost a ubiquitous phase in lepidolite-bearing assemblages.

As a first test, 12 reconnaissance runs were performed on 4 compositions along the join  $\text{PL-SiO}_2$  at 2 kbar. No new crystalline phases other than quartz were observed. The solidus is lowered to about 750°C, above which the assemblage polyolithionite+quartz+liquid+gas appears. Polyolithionite is the liquidus phase up to about 40 wt. percent  $\text{SiO}_2$ ; with



increasing  $\text{SiO}_2$  concentration,  $\beta$ -quartz becomes the liquidus phase. The liquidus surface is very flat on the PL side, but rises abruptly when  $\beta$ -quartz appears on the liquidus. Glasses quenched from liquids in which  $\beta$ -quartz is a primary phase contain rather abundant rounded inclusions of a second glass, suggesting that liquid immiscibility occurs in the silica-rich part of the join. Most importantly, the assemblage polyolithionite + quartz is stable in the subsolidus at temperatures only slightly below the solidus in the quartz-free system. Because this slight lowering could be a result of a diminution in HF fugacity due to dilution of the bulk composition by quartz, it appears that excess  $\text{SiO}_2$  has essentially no effect on lowering the stability of polyolithionite.

On the other hand, phase relations along the join TL- $\text{SiO}_2$  (TL-Q) are complex, in contrast with the pseudobinary PL-Q join. At 2 kbar, the TL-Q join is pseudobinary only at temperatures below about 450°C; at higher temperatures the stable assemblages must be studied in the 6-component system LiAlSiO<sub>4</sub>-KAlSiO<sub>4</sub>-SiO<sub>2</sub>-F-O-H. Neglecting gas components, this system contains two previously investigated sidelines: KAlSiO<sub>4</sub>-SiO<sub>2</sub> (Tuttle and Bowen, 1958; Fudali, 1963), and LiAlSiO<sub>4</sub>-SiO<sub>2</sub> (Roy *et al.*, 1950; Stewart, 1964). The join TL-Q slices a vertical section through the *T-X* prism almost halfway between these two familiar sidelines (Fig. 4); hence a study of phase relations along this join gives considerable information concerning the condensed ternary system KAlSiO<sub>4</sub>-LiAlSiO<sub>4</sub>-SiO<sub>2</sub>. Part of this system is the potash analog of the NaAlSi<sub>3</sub>O<sub>8</sub>-LiAlSiO<sub>4</sub>-SiO<sub>2</sub> system previously investigated by Stewart (1960, 1964).

Note that the join San-Spd intersects the join TL-Q and divides the latter join into silica-saturated and silica-undersaturated parts. Detailed study of phase relations above the solidus was restricted to the silica-saturated part of the TL-Q join.

Starting materials for this series of experiments were either mixtures of trilithionite and quartz in varying proportions or mixtures of appropriate breakdown products. Most runs contained H<sub>2</sub>O as the fluid phase, but a few runs contained extra fluorine, added as dilute aqueous HF (2.7 and 5.2 percent solutions). In certain subsolidus runs, the fugacity of HF was buffered; these experiments will be considered separately.

Quartz reacts with trilithionite to form a large number of assemblages. Figure 5 shows results of experiments for the silica-saturated part of the TL-Q join at 2 kbar. In this section, the minimum of the liquidus falls at TL-Q join at 2kb. In this section, the minimum of the liquidus falls at  $625 \pm 5^\circ\text{C}$ , and at a composition TL<sub>51</sub>Q<sub>49</sub>. The solidus is a flat surface located around 600°C. This temperature must also represent a minimum value for the solidus in the condensed ternary system KAlSiO<sub>4</sub>-LiAlSiO<sub>4</sub>-SiO<sub>2</sub>.

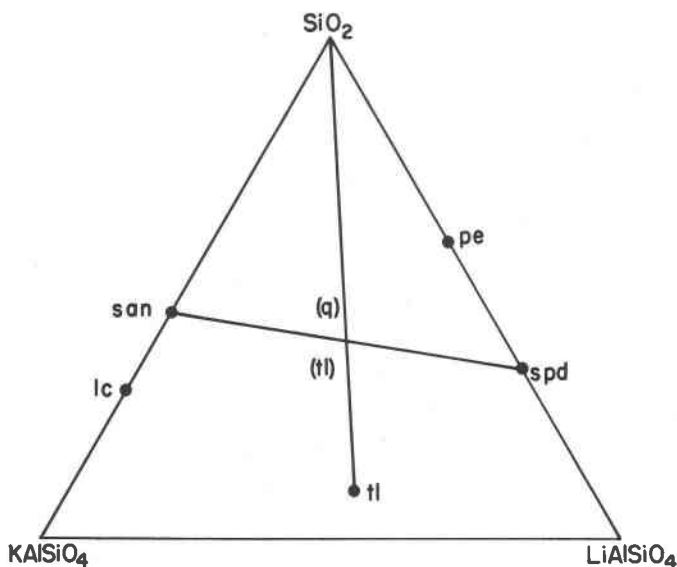


FIG. 4. The condensed system  $\text{KAlSiO}_4(\text{Ks})\text{-LiAlSiO}_4$  (Euc)- $\text{SiO}_2(\text{Q})$ , showing the medial position of the TL-Q join. The join San-Spd divides the TL-Q join into silica-saturated (q) and silica-understaturated (tl) parts. TL: trillithionite, Lc: leucite, Sa: sanidine, Sp: spodumene, Pe: petalite.

The interpretation of the isothermal boundary separating the quartz + liquid field from the quartz + petalite + liquid field is shown in Figure 6. The point  $P$  ( $645^\circ\text{C}$ ,  $\text{TL}_{.45}\text{Q}_{.55}$ ) represents the crossing of the element Liq ( $q$ ,  $pe$ ) over the TL-Q join. Since at a temperature near  $630^\circ\text{C}$  the Sa-Pe join becomes stable, this crossover implies the existence of a eutectic assemblage sanidine + petalite + quartz + liquid + gas stable between  $600$  and  $625^\circ\text{C}$  at some composition within the sanidine-petalite-quartz triangle, but lying on the feldspar side of the TL-Q join. Thus liquidus relations in the system  $\text{KAlSi}_3\text{O}_8\text{-LiAlSiO}_4\text{-SiO}_2$  are similar to those in the system  $\text{NaAlSi}_3\text{O}_8\text{-LiAlSiO}_4\text{-SiO}_2$  (Stewart, 1964) in that the lowest temperature liquids disappear with crystallization of feldspar, petalite, and quartz within analogous compositional triangles. Subsolidus phase relations were investigated using either trillithionite + quartz, sanidine + petalite, or sanidine + spodumene in the presence of both  $\text{H}_2\text{O}$  and HF. Trillithionite + quartz begins to decompose in the presence of  $\text{H}_2\text{O}$  at  $465^\circ\text{C}$  forming sanidine + spodumene while, in 2.7 percent HF solution, no breakdown of trillithionite + quartz is observed at  $522^\circ\text{C}$  after 840 hours. Sanidine + petalite or sanidine + spodumene react to form trillithionite + quartz in the presence of dilute HF solutions at temperatures

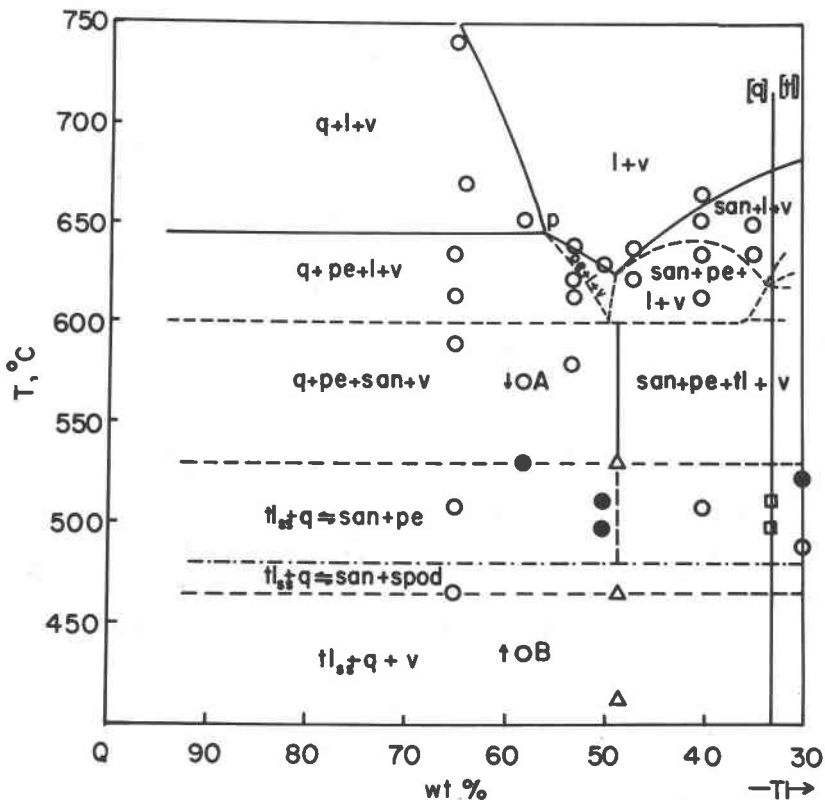
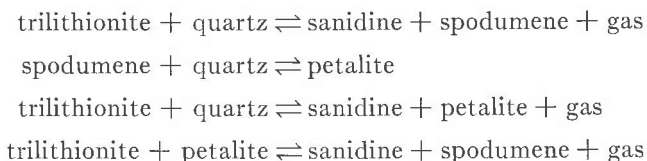


FIG. 5. Silica-saturated part of the join TL-Q at 2 kb total pressure. All runs are unbuffered. Starting materials for all experiments above the solidus was trillithionite (tl) + quartz (q) + water. For subsolidus runs, starting materials are: open circles: trillithionite + quartz + water, closed circles: trillithionite ( $tl_{ss}$ ) + quartz + aqueous HF (2.7 or 5.2 wt percent), triangles: sanidine (san) + petalite (pe) + aqueous HF, squares: sanidine + spodumene (spod) + aqueous HF. The range of temperatures over which the assemblage trillithionite + quartz is stable is a function of the fugacity of HF, and is shown in this diagram between 470°C and 530°C.

as high as 530°C, although the presence of large amounts of amorphous material showed that solution of components by HF had occurred. Because HF becomes a progressively weaker acid at high temperatures (Barnes *et al.*, 1966, p. 409), much of this reaction probably occurred before the run had begun. This problem is one of the most obvious drawbacks of varying HF fugacity by the bulk composition method. For example, in 9.3 percent HF solutions, sanidine + petalite decomposed completely, forming quartz + topaz (?) + amorphous material at 530°C. Thus, it is clear that excess F increases the stability of the assemblage tri-





The experimentally determined sequence of univariant curves is shown as dashed lines in Figure 7 at  $P_{\text{total}} = 2\text{kbar}$ . Triangles represent experiments performed using three fluorine buffers as indicated to define gas compositions (Munoz and Eugster, 1969). The arrows point toward the direction from which equilibrium was approached.

At constant pressure, the degenerate reaction  $\text{spodumene} + \text{quartz} + \text{petalite}$  fixes the temperature of the invariant point, since this reaction is independent of HF. Stewart (1964) reported that petalite has a restricted stability range, decomposing to  $\beta\text{-spodumene}_{\text{ss}} + \beta\text{-quartz}_{\text{ss}}$  at about  $680^{\circ}\text{C}$  at pressures between 2 and 4 kbar, and reacting to form  $\text{spodumene} + \text{quartz}$  when cooled below  $550^{\circ}\text{C}$  at 2kbar. Since, in this investigation, petalite was found to form from the breakdown of  $\text{trilithionite} + \text{quartz}$  below  $510^{\circ}\text{C}$ , the  $\text{spodumene} + \text{quartz} \rightleftharpoons \text{petalite}$  reaction was studied alone, using mixtures of the three reactants as starting materials.

Reaction of  $\text{spodumene} + \text{quartz}$  to form petalite occurred at temperatures as low as  $485^{\circ}\text{C}$ , and traces of spodumene were found in petalite-containing runs at temperatures as high as  $460^{\circ}\text{C}$ . Unfortunately, only three or four crystals of spodumene appeared, even in runs of 1500 hours. The reluctance of spodumene to crystallize at low pressures and temperatures has been commented on previously (Munoz, 1969). For the purpose of this investigation, the reaction  $\text{spodumene} + \text{quartz} \rightleftharpoons \text{petalite}$  has been placed at  $470^{\circ}\text{C}$  at 2kbar.

The three reactions (Pe), (Q), and (Spd) have been extrapolated to intersect at the invariant HF fugacity of about 0.5 bar. Because moderately large uncertainties are associated with the slopes of these curves, and considering probable accuracy limits involved in fluorine buffer calculations, a liberal estimate of error for the invariant HF fugacity is probably one order of magnitude in each direction.

#### CONCLUSIONS AND IMPLICATIONS

The most common occurrence of lepidolite is near the core of Li-enriched granitic pegmatites (lithium pegmatites), where common assemblages are lepidolite-quartz and lepidolite-plagioclase-quartz (Cameron *et al.*, 1949). In any given pegmatite, lepidolite may or may not occur in addition to other Li minerals, most notably spodumene and

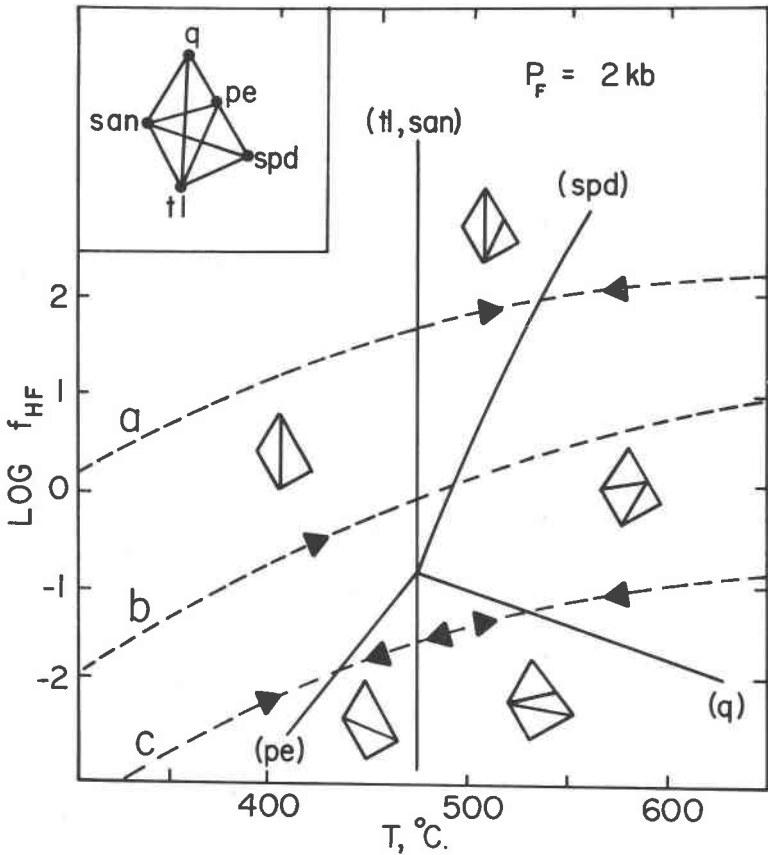


FIG. 7.  $\text{Log } f_{\text{HF}}-T$  showing sequence of univariant curves around the invariant point trillithionite (tl)+sanidine (san)+quartz (q)+petalite (pe)+spodumene (spd)+gas (g) at a total pressure of 2kb. The approximate positions of the univariant curves have been established partly by the temperature of the reaction spodumene+quartz=petalite ( $480^{\circ}\text{C}$ ) and partly using the fluorine buffer technique to locate other curves. All boundaries have been reversed; arrows show direction from which equilibrium was approached. Dashed curves are the fluorine buffer assemblages: (a)  $\text{NNO,OH}(\text{CFG,COHF})$ , (b)  $\text{NNO,OH}(\text{AFSQ,OHF})$ , (c)  $\text{MIC,COH}(\text{QFIC,COHF})$ . For explanation of the notation of fluorine buffers, see Munoz and Eugster (1969).

amblygonite. Most investigators (*e.g.*, Jahns and Burnham, 1961; 1969) believe that these granitic pegmatites originated with magmatic crystallization and evolved by successive crystallization involving both a magma and a supercritical gas phase and finally a gas phase alone. Because of the proximity of lepidolite to the cores of zoned pegmatites, it is probable that most if not all lepidolite forms at subsolidus tempera-

tures which, for pegmatitic magmas, probably means less than 600°C at 2kbar (Jahns and Burnham, 1958).

The melting experiments for the two trioctahedral lepidolite end members clearly show that, in the absence of quartz, lepidolite *could* appear as a liquidus phase if HF fugacity is sufficiently high. Of course, the data behind this statement were obtained from the pure trioctahedral end members polyolithionite and trilithionite; because most natural lepidolites are ternary solid solutions in the system PL-TL-MS, the effect of the MS component on stability must be considered. However, the maximum thermal stability of muscovite is comparable to that of trilithionite (Yoder and Eugster, 1955; Velde, 1966); furthermore, plots of chemical analyses of lepidolite in the ternary system PL-TL-MS show MS to be by far the least abundant component (Munoz, 1968). Thus, if we can assume that the binary solid solution loops lack any minima, then the data obtained from the trioctahedral end members can be applied as stability limits to the ternary solutions.

The supposition that natural lepidolite is almost certainly a subsolidus phase seems, therefore, to be the possible result of three effects: (a) the coupling of quartz-lepidolite reactions, (b) a relatively low level of HF fugacity during the magmatic stages of crystallization, or (c) effect of other components—especially sodium—on the equilibrium. Lack of lithium during the magmatic period does not, in general, provide an alternative explanation, because amblygonite or spodumene is commonly observed in the middle-to-outer zones of zoned Li pegmatites.

The importance of the fugacity of HF in controlling lepidolite phase relations cannot be overemphasized. We do not know what the possible ranges of HF fugacity can be during the course of pegmatite crystallization. Investigations into  $\text{OH} \rightleftharpoons \text{F}$  solid solution in phlogopite suggest that the gas phase in equilibrium with even the most fluorine-rich natural phlogopites did not greatly exceed 0.50 mole percent HF (Munoz and Eugster, 1969). Conceivably, HF concentrations in pegmatite gases could be of the same relatively low magnitude.

The trilithionite-quartz subsolidus reactions provide an excellent model for studying the effect of HF on lepidolite equilibria in silica-saturated pegmatites. For example, consider a lithium pegmatite magma which initially contains a certain amount of HF. As temperature falls, assuming no other fluoride-bearing phases are present, the fugacity of HF will increase (along with an increase in total pressure) due to the crystallization of solid phases. At some temperature, the trace of increasing  $f_{\text{HF}}$  will intersect the maximum stability of lepidolite-quartz (represented by curve Pe-Spd in Fig. 7), and lepidolite will begin to crystallize. In this experimental study, this reaction has been written potash feldspar

+spodumene (or petalite) = trillithionite + quartz. In pegmatites, the analogous reaction would be somewhat more complicated because the phases are not pure; for instance, it is possible to write a balanced equation such as: microcline + spodumene + gas = lepidolite<sub>88</sub> + quartz + an aluminous phase (*e.g.*, topaz, amblygonite). The higher the  $f_{HF}$  at intersection, the higher the temperature at which lepidolite can coexist with quartz, possibly as high as 530°C (at 2kbar) in the pure potash system.

To conclude, the TL-Q join is meant only to be a starting model for lepidolite equilibria in pegmatite systems. A fairly close approach to some lithium pegmatite compositions can be obtained by adding the component NaAlSi<sub>3</sub>O<sub>8</sub> to the KAlSiO<sub>4</sub>-LiAlSiO<sub>4</sub>-SiO<sub>2</sub>-F-O-H system; such a study would be most interesting, but will probably require microprobe techniques for determination of compositions of coexisting feldspar and mica phases.

#### ACKNOWLEDGEMENTS

The bulk of the experimental work described in this paper formed part of the author's Ph.D. dissertation at the Johns Hopkins University, and was supported by the National Science Foundation, GP-1796. Dr. Hans P. Eugster, Dr. David B. Stewart, and Dr. David R. Wones read early drafts of the manuscript and suggested meaningful improvements.

#### APPENDIX

##### *Description and Preparation of Phases Encountered in This Study*

- (1) Polyolithionite, KL<sub>2</sub>AlSi<sub>4</sub>O<sub>10</sub>F<sub>2</sub>: Prepared hydrothermally in >99 percent yield at 2kbar, 780°C from a mix consisting of reagent grade KHCO<sub>3</sub>,  $\gamma$ -Al<sub>2</sub>O<sub>3</sub>, SiO<sub>2</sub> ( $\alpha$ -cristobolite), and LiF. For X-ray power and optical data, see Munoz (1968), pp 1495-1496. Takeda and Burnham (1969) have published the crystal structure of a polyolithionite crystal grown during this investigation. Essentially no hydroxyl is present in polyolithionite.
- (2) Trillithionite, KLi<sub>3/2</sub>Al<sub>3/2</sub>Si<sub>3</sub>AlO<sub>10</sub>(F,OH)<sub>2</sub>: Prepared hydrothermally in >99 percent yield at 2kbar, 650°C from same mix components as above. Mica was always very fine-grained (crystals less than 5  $\mu$ m). The 1M polymorph was used as starting material for all runs. Measurements of the (005) spacing showed that, in the absence of a fluorine buffer, no OH $\rightleftharpoons$ F exchange occurred so long as the mica was held within its stability field.
- (3) Glass: Prepared hydrothermally by holding either polyolithionite or trillithionite above the liquidus and rapidly quenching. Glasses of both compositions are colorless and have essentially identical refractive indices ( $1.494 \pm 0.002$ , measured in Na light). Glasses quenched from PL liquids held at temperatures above 800°C invariably contain spherical inclusions of very fine grained LiF. Because the amount of LiF obtained was dependent on the rate of cooling of the charge, and since the LiF is formed from charges held at temperatures well above the melting point of LiF (870°C at 1 atm.), it is clear that LiF crystallizes during quenching of the charge and is not a stable phase at run temperature. LiF was never observed in TL glasses, but clusters of tiny acicular crystals radiating from a central nucleus were rather common. From optical properties, this "stellate" quench phase is probably eucryptite.

Liquid immiscibility textures (spherical inclusions of one glass in another) were



- commonly quenched from silica-rich compositions on the PL-Q join and were rarely observed at the outer surface of glass pellets of TL composition. In the latter case, the two glasses probably represent a quenching phenomenon.
- (4) Sanidine,  $\text{KAlSi}_3\text{O}_8$ : Sanidine, obtained from incongruent melting of polyolithionite, commonly forms small, almost isotropic anhedral crystals ( $\bar{n}$  = ca. 1.525) which are readily identifiable by X-rays (Borg and Smith, 1969, pp. 696–699).
  - (5) Lithium metasilicate,  $\text{Li}_2\text{SiO}_3$ : Lithium metasilicate was encountered as a breakdown product of polyolithionite in only a few runs and is thought to be metastable at high HF fugacities. It crystallizes as strikingly euhedral acicular to prismatic crystals (uniaxial (+),  $\epsilon$  = 1.61), and is identical to the phase originally described by Austin (1947).
  - (6) Eucryptite,  $\text{LiAlSiO}_4$ : Eucryptite ( $\alpha$ -eucryptite of Roy *et al.*, 1950) forms as a breakdown product of trillithionite at all temperatures and pressures below the liquidus and crystallizes readily from glasses of trillithionite composition above the upper stability limit of the mica. Euhedral crystals with a quartz-like morphology (most common forms: hexagonal prism, rhombohedron, basal pinacoid, and trigonal pyramid) as large as 4 mm were grown, although the average size ranged from 1/10 to 1 mm. Optical properties (uniaxial (+)  $\epsilon$  =  $1.585 \pm 0.005$ , birefringence moderate to high in small crystals) agree with previously described data (Roy *et al.*, *ibid.*), and the X-ray diffractometer trace shows this material to be identical to eucryptite synthesized by Stewart (1960).
  - (7)  $\beta$ -eucryptite ( $\text{LiAlSiO}_4\text{-SiO}_2$ )<sub>ss</sub>: The high temperature polymorph of eucryptite ( $\beta$ -eucryptite of Roy *et al.*, *op. cit.*) was encountered at low pressures and at temperatures above 860°C. The crystals are euhedral to subhedral, generally small (less than 0.1 mm), optically uniaxial (-), and roughly rhombohedral in aspect.  $\omega$  was determined to be  $1.525 \pm 0.005$ , in good agreement with the data of Roy *et al.* previously cited. Commonly, the only X-ray reflection which was observed was the (102) reflection ( $d$  = 3.53 Å), although the (100), ( $d$  = 4.55 Å), and the (114), ( $d$  = 1.91 Å) reflections could rarely be detected. These spacings suggest a composition close to  $\text{LiAlSiO}_4$  (D. B. Stewart, personal communication), but some solid solution toward  $\text{SiO}_2$  is probable (Munoz, 1969).
  - (8) Leucite ( $\text{KAlSi}_2\text{O}_6$ ): Leucite appeared as a decomposition product of trillithionite and was readily recognized by both X-rays and optics. Euhedral leucite crystals as large as 1/2 mm were grown, and the only form observed was the tetragon-trioctahedron (211). The crystals were nearly isotropic, with  $\bar{n}$  =  $1.510 \pm 0.005$ . Inversion twinning was visible on the larger crystals.
  - (9) Kalsilite ( $\text{KAlSiO}_4$ ): Kalsilite (hexagonal form), obtained as a breakdown product of trillithionite, was identified solely on the basis of X-ray reflections (Smith and Tuttle, 1957). Individual crystals were very fine-grained and were commonly coated by aggregates of trillithionite.
  - (10) Spodumene ( $\alpha$ - $\text{LiAlSi}_2\text{O}_6$ ): Spodumene displays typical pyroxene morphology, and X-ray data obtained agrees with Borg and Smith (1969, pp. 253–256). Spodumene was obtained from three sources: (a) as a subsolidus decomposition product of trillithionite+quartz where it appeared as small acicular to prismatic crystals, (b) purified natural spodumene from the Black Hills, South Dakota, (c) synthetic spodumene prepared from glass at 30 kbar, 1200°C (Munoz, 1969).
  - (11) Petalite ( $\text{LiAlSiO}_4$ ): Petalite obtained as a reaction product of trillithionite and quartz occurs as anhedral to slightly bladed crystals. It is identical to the phase described by Deer *et al.* (1963, v. 4, p. 271). For X-ray data, see Borg and Smith (1969, pp. 801–

- 804). Synthetic petalite was prepared hydrothermally at 2kbar, 600°C, from a mix composed of  $\text{Li}_2\text{CO}_3$ ,  $\gamma\text{-Al}_2\text{O}_3$ , and  $\text{SiO}_2$ .
- (12) Quartz ( $\text{SiO}_2$ ): Lake Toxoway quartz was used as a starting material for runs on the Pl-Q and Tl-Q joins. Spacings of quartz obtained from several runs involving a liquid phase showed no change as compared with standard quartz; hence no significant solid solution with  $\text{LiAlSiO}_4$  was detected.

## REFERENCES

- AUSTIN, A. E. (1947) X-ray diffraction data for compounds in systems  $\text{Li}_2\text{O-SiO}_2$  and  $\text{BaO-SiO}_2$ . *J. Amer. Ceram. Soc.* **30**, 218-220.
- BARNES, H. L., H. C. HELGESON, AND A. J. ELLIS (1966) Ionization constants in aqueous solutions, In *Geol. Soc. Amer. Mem.* **97**, 401-413.
- BORG, I. Y., AND D. K. SMITH (1969) Calculated X-ray powder patterns for silicate minerals. *Geol. Soc. Amer. Mem.* **122**, 896 pp.
- CAMERON, E. N., R. H. JAHNS, A. H. McNAIR, AND L. R. PAGE (1949) Internal structure of granitic pegmatites. *Econ. Geol. Monogr.* **2**, 115 pp.
- DEER, W. A., R. A. HOWIE, AND J. ZUSSMAN (1964) *Rock Forming Minerals, Vol. 4, Framework Silicates*. John Wiley and Sons, New York, 270 pp.
- FOSTER, M. D. (1960) Interpretation of the composition of lithium micas. *U.S. Geol. Surv. Prof. Pap.* **354-E**, 115-147.
- FUDALI, R. (1963) Experimental studies bearing on the origin of pseudoleucite and associated problems of alkalic rock systems. *Geol. Soc. Amer. Bull.* **74**, 1101-1126.
- HOUGEN, O. A., AND K. M. WATSON (1946) *Chemical Processes Principles Charts*. John Wiley and Sons, New York, 219 pp.
- ISAACS, T., AND R. ROY (1958) The  $\alpha$ - $\beta$  inversions in eucryptite and spodumene. *Geochim. Cosmochim. Acta* **15**, 213-217.
- JAHNS, R. H. (1955) The study of pegmatities. *Econ. Geol., 50th Anniv. Vol.*, pp. 1026-1130.
- , AND C. W. BURNHAM (1958). Experimental studies of pegmatite genesis: Melting and crystallization of granite and pegmatite (abstr.). *Geol. Soc. Amer. Bull.* **69**, 1592-1593.
- AND ——— (1961) Experimental studies of pegmatite genesis: A model for the crystallization of granitic pegmatites. *Geol. Soc. Amer. Spec. Pap.* **68**, 206-207.
- , AND ——— (1969) Experimental studies of pegmatite genesis: I. A model for the derivation and crystallization of granitic pegmatites. *Econ. Geol.* **64**, 843-864.
- MUNOZ, J. L. (1968) Physical properties of synthetic lepidolites. *Amer. Mineral.* **53**, 1490-1512.
- (1969) Stability relations of  $\text{LiAlSi}_2\text{O}_6$  at high pressures. *Mineral. Soc. Amer. Spec. Pap. No. 2*, 203-209.
- AND H. P. EUGSTER (1969) Experimental control of fluorine reactions in hydrothermal systems. *Amer. Mineral.* **54**, 943-959.
- ROBIE, R. A., AND D. R. WALDBAUM (1968) Thermodynamic properties of minerals and related substances at 298.15°K (25.0°C) and one atmosphere (1.013 bars) pressure and at higher temperatures. *U.S. Geol. Surv. Bull.* **1259**, 256 pp.
- ROY R., D. M. ROY, AND E. F. OSBORN (1950) Compositional and stability relationships among the lithium aluminosilicates: eucryptite, spodumene, and petalite. *J. Amer. Ceram. Soc.* **33**, 152-159.
- SMITH, J. V., AND O. F. TUTTLE (1957) The nepheline-kalsilite system. I. X-ray data for the crystalline phases. *J. Sci.* **255**, 282-305.
- STEWART, D. B. (1960) The system  $\text{LiAlSiO}_4\text{-NaAlSi}_3\text{O}_8\text{-H}_2\text{O}$  at 2000 bars. *Int. Geol. Congr. XXI Session, Norden, 1960. Pt. XVII, Minerals and Genesis of Pegmatites*, pp. 15-30.

- (1964). Petrogenesis and mineral assemblages of lithium-rich pegmatites. (abstr.). *Geol. Soc. Amer. Spec. Pap.* **76**, 159.
- TAKEDA, H., AND C. W. BURNHAM (1969) Fluor-polyolithionite: A lithium mica with nearly hexagonal  $(\text{Si}_2\text{O}_6)^{2-}$  ring. *Mineral. J.* **6**, 102-109.
- TUTTLE, O. F., AND N. L. BOWEN (1958) Origin of granite in the light of experimental studies in the system  $\text{NaAlSi}_3\text{O}_8\text{-KAlSi}_3\text{O}_8\text{-SiO}_2\text{-H}_2\text{O}$ . *Geol. Soc. Amer. Mem.* **74**, 153 pp.
- VELDE, B. (1966) Upper stability of muscovite. *Amer. Mineral.* **51**, 924-929.
- YODER, H. S., AND H. P. EUGSTER (1955) Synthetic and natural muscovites. *Geochim. Cosmochim. Acta* **8**, 225-280.
- WYLLIE, P. J., AND O. F. TUTTLE (1961) Experimental investigation of silicate systems containing two volatile components. Pt. II. The effects of  $\text{WH}_3$  and HF, in addition to  $\text{H}_2\text{O}$  on the melting temperatures of albite and granite. *Amer. J. Sci.* **259**, 128-143.
- Manuscript received, March 26, 1971; accepted for publication, June 10, 1971.*